IEEE Access
Multidisciplinary : Rapid Review : Open Access Journal

Received February 27, 2020, accepted March 5, 2020, date of publication March 10, 2020, date of current version March 23, 2020.

Digital Object Identifier 10.1109/ACCESS.2020.2979735

Comparisons on Kalman-Filter-Based Dynamic State Estimation Algorithms of Power Systems

HUI LIU[1], FEI HU[1], JINSHUO SU[1], XIAOWEI WEI[2], AND RISHENG QIN[3]
[1]School of Electrical Engineering, Guangxi University, Nanning 530004, China
[2]Dongguan Power Supply Bureau, Guangdong Power Grid Corporation Ltd., Dongguan 523003, China
[3]Electric Power Research Institute, Yunnan Power Grid Corporation Ltd., Kunming 650217, China

Corresponding authors: Fei Hu (hufei.cq@foxmail.com) and Jinshuo Su (sjs1205@163.com)

This work was supported in part by the National Natural Science Foundation of China under Grant 51977041 and Grant 61963003, and in part by the Natural Science Foundation for Distinguished Young Scholars of Guangxi under Grant 2018GXNSFFA281006.

ABSTRACT The Kalman-filter-based algorithms as the mainstream algorithms of dynamic state estimation of power systems have been extensively used to provide accurate data for power system applications. However, few comparisons are made to show their advantages and disadvantages. In this paper, four Kalman-filter-based algorithms (i.e., extended Kalman filter, unscented Kalman filter, cubature Kalman filter, and ensemble Kalman filter) are compared to show their differences from implementation complexity, estimation accuracy and calculation efficiency, the resistance to measurement errors, and the sensitivity to system scales. Finally, the simulation results on the 3-machine, 10-machine, and 48-machine power systems show their advantages and disadvantages.

INDEX TERMS Cubature Kalman filter, dynamic state estimation, ensemble Kalman filter, extended Kalman filter, unscented Kalman filter.

I. NOMENCLATURE

$\boldsymbol{a}$	Admittance angle matrix
$\boldsymbol{C}$	Equal weight cubature points vector
$\boldsymbol{D}$	Damping coefficient
$\boldsymbol{e}$	Unit column vector
$\boldsymbol{E}$	EnKF sample set
$\boldsymbol{f}(\cdot)$	State transition function
$\boldsymbol{F}$	Jacobian matrix of state transition function
$\boldsymbol{h}(\cdot)$	Measurement function
$\boldsymbol{H}$	Jacobian matrix of measurement function
$\boldsymbol{I}$	Unit matrix
$\boldsymbol{k}$	Filtering gain
$\boldsymbol{p}_e$	Electromagnetic power of the generator
$\boldsymbol{p}_m$	Mechanical power of the generator
$\boldsymbol{P}_k$	Estimated error covariance
$\boldsymbol{P}_{zz}$	Innovation covariance matrix
$\boldsymbol{P}_{xz}$	The cross-covariance matrix
$\boldsymbol{Q}$	System noise variance
$\boldsymbol{R}$	Measurement noise variance
$\boldsymbol{S}$	Weighted Sigma points vector
$\boldsymbol{T}$	Inertia constant of the generator
$\boldsymbol{u}$	Constant control vector
$\boldsymbol{v}$	Measurement noise vector
$\boldsymbol{V}$	Voltage amplitude
$\boldsymbol{w}$	System noise vector
$\boldsymbol{W}_c$	Weight vectors of covariance
$\boldsymbol{W}_m$	Weight vectors of mean
$\boldsymbol{x}$	State vector
$\boldsymbol{Y}$	Reduced node admittance matrix
$\boldsymbol{z}$	Measurement vector
$\boldsymbol{\delta}$	Generator power angle
$\boldsymbol{\omega}$	Generator speed
$\boldsymbol{\omega}_s$	Generator reference speed
$\boldsymbol{\omega}_\delta$	System noise vector of generator power angle
$\boldsymbol{\omega}_\omega$	System noise vector of generator speed
h	Difference step size
i, j	The ith/jth generator
k	Current time
n	Number of generators
n_{en}	Number of samples
N	Number of times
$\alpha, \beta, \eta, \lambda, l$	Setting parameters of UKF
$\wedge, ^{-}$	Estimated/prediction value of variables

The associate editor coordinating the review of this manuscript and approving it for publication was Wuhui Chen.

II. INTRODUCTION

Power system state estimation as one of the keys of the energy management system is paid much attention to, as it can grasp the real-time state of the power system by filtering the measurement data that cannot represent the actual state of power systems due to the errors such as measurement and transmission errors. In particular, the dynamic state estimation (DSE) of power systems has become a very 'hot' topic in recent years [1]–[3]. The mainstream DSE algorithms of power systems, such as extended Kalman Filter (EKF) and unscented Kalman filter (UKF), are developed based on Kalman-filter (KF) theory [4], [5] and has been studied extensively.

The EKF algorithm as one of the most common KF-based nonlinear algorithm is based on the Taylor series expansion. In [6], the feasibility of EKF to power system applications is addressed based on the data from the synchronized phasor measurement unit (PMU), and at the same time, the estimation performance of EKF is discussed in a 3-machine 9-bus power system from sampling frequency, measurement error, and the influence of fault and load change. A distributed EKF method was proposed based on the Wide Area Measurement System (WAMS) in [7], for which, the generator rotor motion equation is decoupled from the external network. However, because of ignoring the higher-order term of Taylor expansion, EKF causes a large truncation error and results in a decrease in filter performance in the case of strong nonlinearity. Adaptive interpolation and adaptive multi-step prediction are respectively proposed in [8] and [9] and can reduce the influence of nonlinearity on the estimation accuracy of EKF, but the complexity of the algorithms increases greatly. The EKF algorithm achieves nonlinear state estimation by approximating nonlinear function, while the other KF-based algorithms, such as UKF, cubature Kalman filter (CKF), and ensemble Kalman filter (EnKF), are to approximate the posterior probability distribution of random variables.

While using the set of weighted sigma points transferred by nonlinear function, the UKF algorithm can combine the unscented transformation and KF to approximate the posterior probability distribution of random variables without calculating the Jacobian matrix [10]–[17]. In [13], by combining WAMS data and the measurement data from the supervisory control and data acquisition system, a UKF-based DSE method of power systems is proposed in the case of mixed measurement and verified on a 4-machine system. In [15], a robust generalized maximum-likelihood UKF is provided to handle unknown statistics, measurement noises, and bad measurements. However, as the variable dimension and nonlinearity increase, the algorithm cannot be recursive due to the difficulty in maintaining the positive definiteness of the covariance matrix of UKF. To improve the numerical stability of UKF, a symmetric positive semi-definite matrix, which is closest to the Frobenius-norm of the original matrix, is generated to ensure the positive semi-definiteness of the covariance matrix during iteration [17].

To approximate the posterior probability distribution of random variables, UKF uses the set of weighted sigma points transferred by nonlinear function, while CKF considers the set of equal weight cubature points generated according to spherical-radial rule [18]–[22]. As CKF is not sensitive to variable dimensions, it is not necessary to set cubature point parameters [18]. With the measurement data from PMU and remote terminal unit, CKF was applied to address the DSE of power systems in [19], and its superiority is demonstrated in the 30-bus and 246-bus power system compared with EKF and UKF. In [20], a robust CKF method is proposed to estimate generator dynamics and shows that the resistance to bad data can be improved at the cost of computational efficiency. In [21], CKF and Huber's M-estimation are combined to detect outliers and gross errors.

Different from the deterministic sampling strategy of UKF and CKF, the EnKF algorithm uses random sampling to generate the sample set that can be adjusted according to actual requirements [23]–[29]. In this condition, the larger the sample set is, the higher the approximate accuracy is. In [23], EnKF was used for the DSE of power systems and addressed from the accuracy of the initial value, model error, and the sensitivity to sampling frequency. EnKF was also used to estimate the power system harmonic state in [25] and to calibrate the generator parameters to reduce the mismatch between PMU measurement and the generator state in [27].

The four KF-based algorithms mentioned above have been widely used in the DSE of power systems. As the KF theory was proposed based on the Gaussian distribution noise to keep an optimal estimation with the unbiased minimum variance [4], [5], the four KF-based algorithms remain this distribution. The existing work has shown that the non-Gaussian noises will result in the bad estimation performance of these algorithms. For instance, in [3], non-Gaussian noises make the estimation of UKF severely deviate from the true values; in [21], it has been shown that the estimation of CKF will be distorted, while Cauchy noise and Laplace noise are used to assess its performance. Therefore, to show their advantages and disadvantages, the four KF-based algorithms are compared on the basis of Gaussian distribution. The main contributions are shown, as follows:

- The four KF-based DSE algorithms are summarized and compared to show their complexity from Jacobian matrix calculation, parameter setting, and the sample size.
- The advantages and disadvantages of the four algorithms are shown from the calculation speed and accuracy, the resistance to error, and the sensitivity to system scales.

The remainder of this paper is arranged as follows. In Section II, the model of DSE is provided. The four KF-based algorithms are introduced and compared in Section III, and simulation results are presented in Section IV. Finally, the conclusion is drawn in Section V.

III. THE MODEL OF DYNAMIC STATE ESTIMATION

A. THE THEORY OF DYNAMIC STATE ESTIMATION

The equations of state and measurement for nonlinear systems have the following expression:

$$\begin{cases} \boldsymbol{x}_k = \boldsymbol{f}(\boldsymbol{x}_{k-1}, \boldsymbol{u}_{k-1}) + \boldsymbol{w}_{k-1} \\ z_k = \boldsymbol{h}(\boldsymbol{x}_k) + \boldsymbol{v}_k \end{cases} \tag{1}$$

where $\boldsymbol{x}_k$ is n dimensional state vector, z_k is m dimensional measurement vector, the subscript k represents time, and $\boldsymbol{u}_{k-1}$ is the control vector at time $k-1$; $\boldsymbol{f}(\cdot)$ and $\boldsymbol{h}(\cdot)$ are the state transition function and measurement function, respectively; $\boldsymbol{w}$ and $\boldsymbol{v}$ are system noise vector and measurement noise vector, respectively, which are usually assumed to be uncorrelated Gaussian noise in (2).

$$\begin{cases} \boldsymbol{w} \sim N(0, \boldsymbol{Q}) \\ \boldsymbol{v} \sim N(0, \boldsymbol{R}) \end{cases} \tag{2}$$

where $\boldsymbol{Q}$ and $\boldsymbol{R}$ are the system noise variance and measurement noise variance, respectively.

The dynamic state estimation is to get the estimated value $\hat{\boldsymbol{x}}_k$ by appropriately correcting the prediction value $\boldsymbol{x}_k^-$, while obtaining the measurement z_k, as shown in (3).

$$\begin{cases} \boldsymbol{x}_k^- = \boldsymbol{f}(\hat{\boldsymbol{x}}_{k-1}, \boldsymbol{u}_{k-1}) \\ \hat{\boldsymbol{x}}_k = \boldsymbol{x}_k^- + \boldsymbol{k}_k(z_k - \boldsymbol{h}(\boldsymbol{x}_{k-1}^-)) \end{cases} \tag{3}$$

Therefore, with the measurement vector z_k and the estimated value $\hat{\boldsymbol{x}}_{k-1}$, to calculate the filtering gain $\boldsymbol{k}_k$, we can minimize the estimated error covariance as

$$\min \boldsymbol{P}_k = E((\boldsymbol{x}_k - \hat{\boldsymbol{x}}_k)(\boldsymbol{x}_k - \hat{\boldsymbol{x}}_k)^T) \tag{4}$$

where $\boldsymbol{x}_k$ is a true value vector.

Note that for the nonlinear equation (1), it is hard to find the analytical solution of (4), but KF can provide an optimal solution of the linear equation, as shown in (5) [30]:

$$\boldsymbol{k}_k = \boldsymbol{P}_{xz}(\boldsymbol{P}_{zz} + \boldsymbol{R})^{-1} \tag{5}$$

When KF is extended to a nonlinear system, approximating the innovation covariance matrix $\boldsymbol{P}_{zz}$ and the cross-covariance matrix $\boldsymbol{P}_{xz}$ is the essential difference among the four KF-based algorithms discussed in Section III.

B. THE MODEL OF DYNAMIC STATE ESTIMATION OF POWER SYSTEMS

The equation of generator rotor motion has the following expression:

$$\begin{cases} \dfrac{d\boldsymbol{\delta}}{dt} = \boldsymbol{\omega}_s(\boldsymbol{\omega} - 1) \\ \dfrac{d\boldsymbol{\omega}}{dt} = \dfrac{1}{\boldsymbol{T}}(\boldsymbol{p}_m - \boldsymbol{p}_e - \boldsymbol{D}(\boldsymbol{\omega} - 1)) \end{cases} \tag{6}$$

where $\boldsymbol{\delta}$ and $\boldsymbol{\omega}$ represent the generator power angle and speed respectively, $\boldsymbol{\omega}_s$ is the reference speed, $\boldsymbol{T}$ is the inertia constant of the generator, $\boldsymbol{p}_m$ is the mechanical power of the generator, $\boldsymbol{p}_e$ is the electromagnetic power of the generator, and $\boldsymbol{D}$ is the damping coefficient.

The equation (6) can also be re-written as:

$$\begin{cases} \boldsymbol{\delta}_k = \boldsymbol{\delta}_{k-1} + \boldsymbol{\omega}_s(\boldsymbol{\omega}_{k-1} - 1) + \boldsymbol{\omega}_\delta \\ \boldsymbol{\omega}_k = \boldsymbol{\omega}_{k-1} + h * (\boldsymbol{p}_m - \boldsymbol{p}_{e,k-1} - \boldsymbol{D}(\boldsymbol{\omega} - 1))/\boldsymbol{T} + \boldsymbol{w}_\omega \end{cases} \tag{7}$$

where h is the difference step size, k represents time, $\boldsymbol{\omega}_\delta$ and $\boldsymbol{\omega}_\omega$ correspond to the system noise in (1). In a multi-machine system, the electromagnetic power $\boldsymbol{p}_e$ at time k satisfies

$$\boldsymbol{p}_{ek}^i = \boldsymbol{V}_i \sum_{j=1}^{n} \boldsymbol{Y}_{ij} \boldsymbol{V}_j cos(\boldsymbol{\delta}_{ik} - \boldsymbol{\delta}_{jk} - \boldsymbol{\alpha}_{ij}) \tag{8}$$

where $\boldsymbol{Y}$ represents the reduced node admittance matrix, i represents the generator number, and $\boldsymbol{\alpha}_{ij}$ represents the admittance angle. The generator power angle and speed are considered as the measurement z_k, i.e.,

$$z_k = [\boldsymbol{\delta}_k \quad \boldsymbol{\omega}_k] \tag{9}$$

The constant control vector $\boldsymbol{u}_k$ is:

$$\boldsymbol{u}_k = [\boldsymbol{P}_m \quad \boldsymbol{V}] \tag{10}$$

IV. THE FOUR KF-BASED ALGORITHMS

A. EKF ALGORITHM

While linearizing (1) by using the first-order Taylor expansion to obtain the analytical solution (5), the steps of EKF include prediction step and the filtering step, as follows.

Prediction step:

$$\begin{cases} \boldsymbol{x}_k^- = \boldsymbol{f}(\boldsymbol{x}_{k-1}, \boldsymbol{u}_{k-1}), \quad k \geq 1 \\ \boldsymbol{P}_k^- = \boldsymbol{F}_{k-1}\boldsymbol{P}_{k-1}\boldsymbol{F}_{k-1}^T + \boldsymbol{Q} \end{cases} \tag{11}$$

Filtering step:

$$\begin{cases} \boldsymbol{P}_{zz} = \boldsymbol{H}_k \boldsymbol{P}_k^- \boldsymbol{H}_k^T \\ \boldsymbol{P}_{xz} = \boldsymbol{P}_k^- \boldsymbol{H}_k^T \\ \boldsymbol{k}_k = \boldsymbol{P}_{xz}(\boldsymbol{P}_{zz} + \boldsymbol{R})^{-1} \\ \hat{\boldsymbol{x}}_k = \boldsymbol{x}_k^- + \boldsymbol{k}_k(z_k - \boldsymbol{h}(\boldsymbol{x}_k^-)) \\ \boldsymbol{P}_k = (\boldsymbol{I} - \boldsymbol{k}_k \boldsymbol{H}_k)\boldsymbol{P}_k^- \end{cases} \tag{12}$$

where $\boldsymbol{P}_k$ is the covariance matrix of the estimated value, $\boldsymbol{P}_k^-$ is the covariance matrix of the predicted value $\boldsymbol{x}_k^-$, and $\boldsymbol{H}_k$ and $\boldsymbol{F}_k$ are subjected to (13).

$$\boldsymbol{H}_k = \frac{d\boldsymbol{h}}{d\boldsymbol{x}}|_{\boldsymbol{x}_k^-}, \quad \boldsymbol{F}_k = \frac{d\boldsymbol{f}}{d\boldsymbol{x}}|_{\boldsymbol{x}_{k-1}} \tag{13}$$

The EKF has been extensively used because of its simple steps. However, solving the Jacobian matrix (13) is greatly complicated for large-scale systems or complex equations. Besides, the truncation error will increase due to ignoring the higher-order terms of Taylor expansion, which degrades or even diverges the estimation performance of the system with the strong nonlinearity [17].

B. UKF ALGORITHM

By combining unscented transformation and KF, UKF generates a set of weighted Sigma points to approximate the state mean and covariance matrix in (5). Compared with EKF, UKF does not calculate the Jacobian matrix and simultaneously shows higher approximation accuracy, the steps of which are as follows [17].

The $n * (2n + 1)$-dimension weighted Sigma points are generated by:

$$\boldsymbol{S}_{k-1} = \boldsymbol{x}_{k-1} * \boldsymbol{e}^T + \eta \left[0_{n,1} \ \sqrt{\boldsymbol{P}_{k-1}} \ -\sqrt{\boldsymbol{P}_{k-1}} \right] \tag{14}$$

Prediction step:

$$\begin{cases} \boldsymbol{S}_k^- = \boldsymbol{f}(\boldsymbol{S}_{k-1}, \boldsymbol{u}_{k-1}) \\ \boldsymbol{x}_k^- = \sum_{i=0}^{2n} \boldsymbol{W}_m^i * \boldsymbol{S}_{i,k}^- \\ \boldsymbol{P}_k^- = \sum_{i=0}^{2n} \boldsymbol{W}_c^i (\boldsymbol{S}_{i,k}^- - \boldsymbol{x}_k^-)(\boldsymbol{S}_{i,k}^- - \boldsymbol{x}_k^-)^T + \boldsymbol{Q} \\ \boldsymbol{S}_{xk}^- = \boldsymbol{x}_k^- * \boldsymbol{e}^T + \eta \left[0_{n,1} \ \sqrt{\boldsymbol{P}_{k-1}} \ -\sqrt{\boldsymbol{P}_{k-1}} \right] \\ \boldsymbol{S}_{yk}^- = \boldsymbol{h}(\boldsymbol{S}_{xk}^-) \\ \boldsymbol{y}_k^- = \sum_{i=0}^{2n} \boldsymbol{W}_m^i * \boldsymbol{S}_{i,yk}^- \end{cases} \tag{15}$$

Filtering step:

$$\begin{cases} \boldsymbol{P}_{zz} = \sum_{i=1}^{2n} \boldsymbol{W}_c^i (\boldsymbol{S}_{yk}^- - \boldsymbol{y}_k^-)(\boldsymbol{S}_{yk}^- - \boldsymbol{y}_k^-)^T \\ \boldsymbol{P}_{xz} = \sum_{i=0}^{2n} \boldsymbol{W}_c^2 (\boldsymbol{S}_{i,k}^- - \boldsymbol{x}_k^-)(\boldsymbol{S}_{yk}^- - \boldsymbol{y}_k^-)^T \\ \boldsymbol{k}_k = \boldsymbol{P}_{xz}(\boldsymbol{P}_{zz} + \boldsymbol{R})^{-1} \\ \hat{\boldsymbol{x}}_k = \boldsymbol{x}_k^- + \boldsymbol{k}_k(z_k - \boldsymbol{y}_k^-) \\ \boldsymbol{P}_k = \boldsymbol{P}_k^- - \boldsymbol{k}_k(\boldsymbol{P}_{zz} + \boldsymbol{R})\boldsymbol{k}_k^T \end{cases} \tag{16}$$

where $\boldsymbol{e}$ is the unit column vector; $\boldsymbol{W}_m$ and $\boldsymbol{W}_c$ are the weight vectors of mean and covariance respectively, subjected to:

$$\begin{cases} \boldsymbol{W}_m^0 = \dfrac{\lambda}{n+\lambda} \\ \boldsymbol{W}_m^i = \dfrac{\lambda}{2(n+\lambda)} \quad i = 1 \cdots 2n \\ \boldsymbol{W}_c^0 = \dfrac{\lambda}{n+\lambda} + (1 - \alpha^2 + \beta) \\ \boldsymbol{W}_c^i = \dfrac{1}{2(n+\lambda)} \quad i = 1 \cdots 2n \end{cases} \tag{17}$$

and $\eta = \sqrt{n+\lambda}$, $\beta \geq 0$. The scale parameter satisfies $\lambda = \alpha^2 (n + l) - n$, where α and l are constants, $1 \geq \alpha > 0$, and $l \geq 0$.

Compared with EKF, the covariance calculation is more complex, although it is not necessary for UKF to calculate the Jacobian matrix. At the same time, UKF needs to set the parameter $\boldsymbol{\alpha}$, β, and l to modify the weight of Sigma points, but the parameter setting lacks reference, which limits its popularization.

C. CKF ALGORITHM

Because of using the spherical radial rule to generate equal weight cubature points set, CKF has the following steps [19].

The $n * 2n$-dimension equal weight cubature points are generated by:

$$\boldsymbol{C}_{k-1} = \boldsymbol{x}_{k-1} * \boldsymbol{e}^T + \sqrt{n} \left[\sqrt{\boldsymbol{P}_{k-1}} \ -\sqrt{\boldsymbol{P}_{k-1}} \right] \tag{18}$$

Prediction step:

$$\begin{cases} \boldsymbol{C}_k^- = \boldsymbol{f}(\boldsymbol{C}_{k-1}, \boldsymbol{u}_{k-1}) \\ \boldsymbol{x}_k^- = \dfrac{1}{2n} \sum_{i=1}^{2n} \boldsymbol{C}_{i,k}^- \\ \boldsymbol{P}_k^- = \sum_{i=1}^{2n} (\boldsymbol{C}_{i,k}^- - \boldsymbol{x}_k^-)(\boldsymbol{C}_{i,k}^- - \boldsymbol{x}_k^-)^T + \boldsymbol{Q} \end{cases} \tag{19}$$

Filtering step:

$$\begin{cases} \boldsymbol{C}_{xk}^- = \boldsymbol{x}_k^- * \boldsymbol{e}^T + \sqrt{n} \left[\sqrt{\boldsymbol{P}_k^-} \ -\sqrt{\boldsymbol{P}_k^-} \right] \\ \boldsymbol{C}_{yk}^- = \boldsymbol{h}(\boldsymbol{C}_{xk}^-) \\ \boldsymbol{y}_k^- = \dfrac{1}{2n} \sum_{i=1}^{2n} \boldsymbol{C}_{i,yk}^- \\ \boldsymbol{P}_{zz} = \dfrac{1}{2n} \sum_{i=1}^{2n} (\boldsymbol{C}_{yk}^- - \boldsymbol{y}_k^-)(\boldsymbol{C}_{yk}^- - \boldsymbol{y}_k^-)^T \\ \boldsymbol{P}_{xz} = \dfrac{1}{2n} \sum_{i=1}^{2n} (\boldsymbol{C}_{i,k}^- - \boldsymbol{x}_k^-)(\boldsymbol{C}_{yk}^- - \boldsymbol{y}_k^-)^T \\ \boldsymbol{k}_k = \boldsymbol{P}_{xz}(\boldsymbol{P}_{zz} + \boldsymbol{R})^{-1} \\ \hat{\boldsymbol{x}}_k = \boldsymbol{x}_k^- + \boldsymbol{k}_k(z_k - \boldsymbol{y}_k^-) \\ \boldsymbol{P}_k = \boldsymbol{P}_k^- - \boldsymbol{k}_k(\boldsymbol{P}_{zz} + \boldsymbol{R})\boldsymbol{k}_k^T \end{cases} \tag{20}$$

As shown in (17), for UKF, the weight of the sample center point is larger than that of other sampling points. Therefore, the closer the sample center point is to the true value, the higher the approximate accuracy is. In contrast, for CKF, there is no sampling center point, and the same weight is kept for all sampling points. Therefore, the sampling strategy of CKF is more conservative.

D. ENKF ALGORITHM

Unlike the deterministic sampling strategy of UKF and CKF, EnKF generates a great number of sample set according to the prior distribution of random variables. The larger the sample set is, the higher the approximation accuracy is, but the calculation burden will increase significantly. The steps of EnKF are as follows [23].

When $k = 1$, the sample set is generated by:

$$\boldsymbol{E}_s = \boldsymbol{x}_0 * \boldsymbol{e}^T + \boldsymbol{P}_0 * \mathrm{randn}(2n, n_{en}) \tag{21}$$

TABLE 1. Complexity comparison of four methods.

algorithms	EKF	CKF	EnKF	UKF
Jacobian matrix calculation	Yes	No	No	No
The number of setting parameters	3	3	4	6
The size of sample	/	$2n$	$>n$	$2n+1$

Prediction step:

$$\begin{cases} \boldsymbol{E}_s^- = \boldsymbol{f}(\boldsymbol{E}_s, \boldsymbol{u}_{k-1}) + \boldsymbol{Q} * \mathrm{randn}(2n, n_{en}) \\ \boldsymbol{z}_k^- = \boldsymbol{h}(\boldsymbol{E}_s^-, \boldsymbol{u}_{k-1}) \\ \boldsymbol{x}_k^- = \dfrac{1}{n_{en}} \sum\limits_{i=1}^{n_{en}} \boldsymbol{E}_s^{i-} \\ \boldsymbol{y}_k^- = \dfrac{1}{n_{en}} \sum\limits_{i=1}^{n_{en}} \boldsymbol{z}_k^{i-} \end{cases} \tag{22}$$

Filtering step:

$$\begin{cases} \boldsymbol{P}_{zz} = \dfrac{1}{n_{en}} \sum\limits_{i=1}^{n_{en}} (\boldsymbol{z}_k^{i-} - \boldsymbol{y}_k^-)(\boldsymbol{z}_k^{i-} - \boldsymbol{y}_k^-)^T \\ \boldsymbol{P}_{xz} = \dfrac{1}{n_{en}} \sum\limits_{i=1}^{n_{en}} (\boldsymbol{E}_s^{i-} - \boldsymbol{x}_k^-)(\boldsymbol{z}_k^{i-} - \boldsymbol{y}_k^-)^T \\ \boldsymbol{k}_k = \boldsymbol{P}_{xz}(\boldsymbol{P}_{zz} + \boldsymbol{R})^{-1} \\ \boldsymbol{E}_z = \boldsymbol{z}_k + \boldsymbol{R} * \mathrm{randn}(2n, n_{en}) \\ \hat{\boldsymbol{x}}_k = \boldsymbol{E}_s^- + \boldsymbol{k}_k(\boldsymbol{E}_z - \boldsymbol{z}_k^-) \end{cases} \tag{23}$$

where n_{en} is the number of samples, which is usually not below the dimension of variables.

E. COMPARISONS OF FOUR KF-BASED METHODS

As shown in Table 1, the four KF-based algorithms are compared from the Jacobian matrix, the number of setting parameters, and the size of sample.

From Table 1, EKF needs to calculate the Jacobian matrix, while CKF, EnKF, and UKF do not consider the Jacobian matrix. This means that the computation burden of EKF is heavier than that of CKF, EnKF, and UKF, especially for the highly complicated system. Regarding setting parameters, the more the number of setting parameters is, the more difficult determining parameter values for the current system and error distribution is. Therefore, it is harder for UKF to set parameter values in comparison to EKF, CKF, and EnKF. For EKF, the sample is not considered due to using the Taylor expansion. In contrast, the sample set must be used to achieve the estimation for CKF, EnKF, and UKF. There is no standard for determining the EnKF sample size, but the trial and error on the sample size can be used to ensure the calculation efficiency and estimation accuracy of EnKF. Compared with EnKF, the sample sizes of CKF and UKF are dependent on the size of nonlinear systems.

V. SIMULATIONS AND DISCUSSIONS

Under the MATLAB R2016a environment, the simulations are performed with a computer with an Intel Core i7-7700 CPU and 8 GB memory. To imitate the field PMU dada, we here superimpose the Gaussian distribution noises into the data from the Power System Toolbox [31] which are widely used in the literature such as [15], [17]. The parameters are set in detail, as follows.

a. The sampling frequency of PMU is 50Hz, and the measurements include the generator power angle and speed;
b. A three-phase ground fault occurs at 0.1 s, and the fault is set at the first end of the line with the largest branch power flow and removed after 0.18 s;
c. The initial covariance matrix $\boldsymbol{P}_0$ of the four algorithms is a diagonal matrix with the diagonal elements of 10^{-6}, the system noise covariance matrix $\boldsymbol{Q}$ is a diagonal matrix with the diagonal elements of 0.01^2, and the diagonal elements of the measurement noise covariance matrix $\boldsymbol{R}$ are set to 0.01 for power angle and 0.001 for generator speed.

Besides, we assume that for UKF, $\alpha = 1, \beta = 2, l = 3-n$, while EnKF has the sample size of $n_{en} = 200$.

A. ESTIMATION ACCURACY AND CALCULATION EFFICIENCY

The root-mean-square error is defined as the comparison standard of the estimated accuracy of the four algorithms, as follows.

$$e_x = \sqrt{\frac{\sum\limits_{i=1}^{n} \sum\limits_{k=1}^{N} (\boldsymbol{x}_{i,k}^{est} - \boldsymbol{x}_{i,k}^{true})^2}{nN}} \tag{24}$$

where n indicates the number of generators, N is the number of times, and $\boldsymbol{x}_{i,k}^{est}$ and $\boldsymbol{x}_{i,k}^{true}$ represent the estimated and true values of the ith generator at time k, respectively.

As shown in Fig. 1, the four KF-based algorithms can show good estimation results on a 3-machine 9-bus system. However, the estimation accuracy and calculation efficiency of the four algorithms will change significantly with the increase of the system size, as illustrated in Fig. 2 and Fig. 3.

The estimation accuracy of UKF and CKF is similar but better than that of EKF and EnKF. With the increase of the system scale, CKF, EnKF, and UKF can keep the relatively stable estimation performance for all scale systems, as shown in Fig. 2. However, the estimation accuracy of EKF decreases dramatically for the 48-machine power system due to the truncation error of the Taylor expansion.

For the calculation efficiency, EKF decreases slightly with the increase of system scale, while CKF, UKF, and EnKF decrease dramatically, as shown in Fig. 3. The detailed comparison results are shown in Table 3-Table 5 in the Appendix.

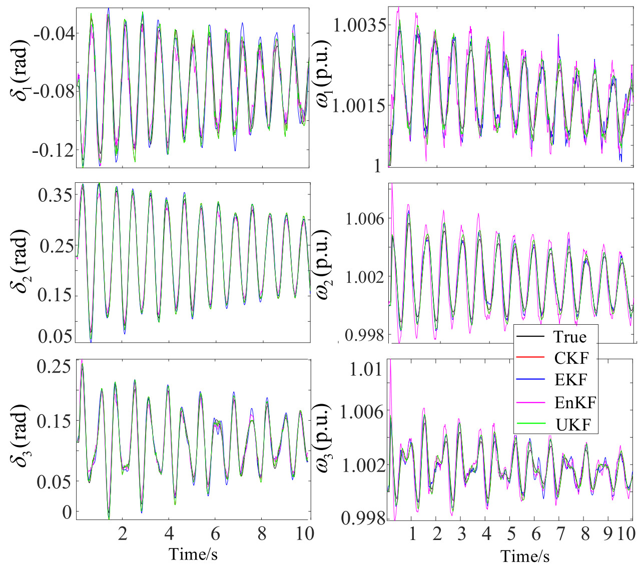

FIGURE 1. Estimations on a 3-machine 9-bus system.

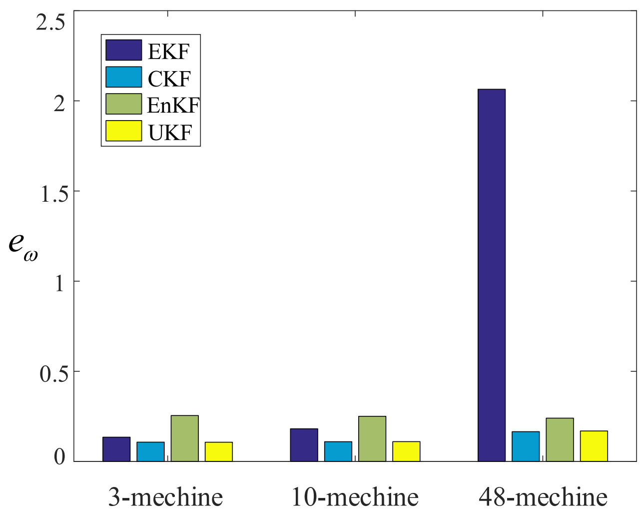

FIGURE 2. Estimation accuracy for different scale systems.

B. THE RESISTANCE TO MEASUREMENT ERRORS

Measurement errors are inevitable, because the measuring accuracy is affected by temperature, instrument aging, and interference, etc. The resistance ability to measurement errors is one of the important indicators to evaluate the effectiveness of the algorithm. The decline of measurement level is imitated by increasing the error standard deviation R_z, which is superimposed on the true value.

As shown in Fig. 4, the estimation performance of the four KF-based algorithms decreases with the increase of measurement error. As the truncation error of the Taylor expansion increases with errors, EKF shows the worst performance in estimation accuracy. Compared with EnKF, UKF and CKF with the similar estimation results achieve better estimation accuracy. Please see the detailed data in Table 6 and Table 7 in the Appendix.

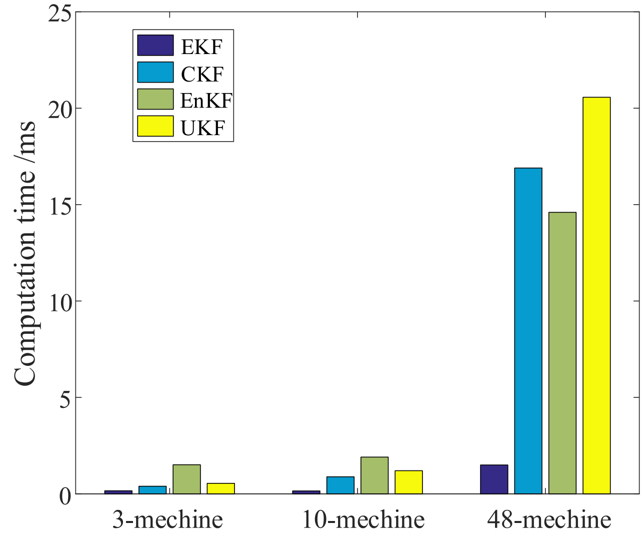

FIGURE 3. Calculation efficiency for different scale systems.

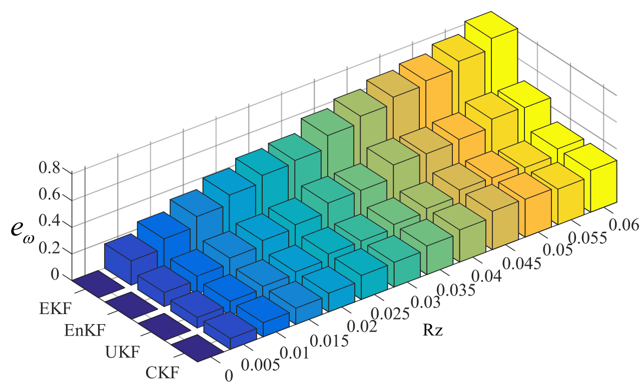

FIGURE 4. Estimation accuracy for different error standard deviations.

C. THE SENSITIVITY TO SYSTEM SCALES

As shown in Fig. 2, the estimation accuracy of EKF drops sharply for the 48-machine system. This is because the estimation results of some generators are divergent due to the large truncation error of the Taylor expansion, as illustrated in Fig. 5. Compared with EnKF, CKF and UKF can still achieve good estimation results.

As the root-mean-square error e_x cannot directly reflect the divergence of the estimation results of each generator, a coefficient index R_{xy} is introduced, as follows.

$$R_{xy} = \frac{\sum_{i=1}^{n} (\boldsymbol{x}_i - \bar{x})(\boldsymbol{y}_i - \bar{y})}{\sqrt{\sum_{i=1}^{n} (\boldsymbol{x}_i - \bar{x})^2 \sum_{i=1}^{n} (\boldsymbol{y}_i - \bar{y})^2}} \tag{25}$$

where $\boldsymbol{x}_i$ and $\boldsymbol{y}_i$ are the estimated values and real values respectively, $\bar{x}$ and $\bar{y}$ are their corresponding mean values, and R_{xy} satisfies $0 < R_{xy} < 1$.

Note that, the closer the value of R_{xy} is to 1, the stronger the correlation between $\boldsymbol{x}$ and $\boldsymbol{y}$ is, and the better estimation

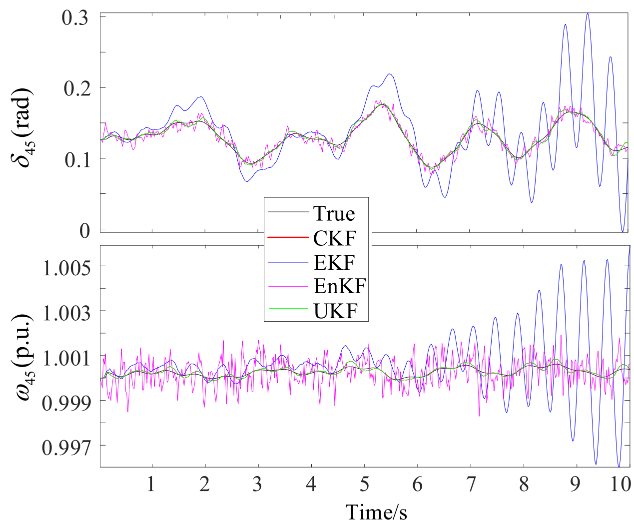

FIGURE 5. Estimation results of the 45th generator in a 48-machine power system.

TABLE 2. The unqualified variables for four algorithms.

Algorithm	EKF	CKF	EnKF	UKF
3-machine system	0	0	0	0
10-machine system	0	0	0	0
48-machine system	11	2	7	2

TABLE 3. Precision and computation efficiency of four methods on a 3-machine 9-bus system.

Algorithms	EKF	CKF	EnKF	UKF
e_δ	0.0075	0.0063	0.0068	0.0063
e_ω	0.1347	0.1068	0.2545	0.1065
Computation time/ms	0.1582	0.3936	1.5088	0.5466

performance is. If $R_{xy} < 0.8$, the estimation value is considered as unqualified. The number of unqualified variables is used to evaluate the performance of the algorithms.

As illustrated in Table 2, for the 3-machine system and the 10-machine system, there is no estimation distortion. However, in the 48-machine system, EKF has the most amount of distortion, while UKF and CKF have the least distortion. Therefore, UKF and CKF have less sensitivity to the system size, compared with EnKF and EKF.

VI. CONCLUSION

In this paper, to show the advantages and disadvantages of the four KF-based mainstream algorithms (i.e., EKF, UKF, EnKF, and CKF), we compare them from algorithm complexity, calculation speed and accuracy, the resistance to measurement errors, and the sensitivity to system scales.

TABLE 4. Precision and computation efficiency of four methods on a 10-machine 39-bus system.

Algorithms	EKF	CKF	EnKF	UKF
e_δ	0.0127	0.0095	0.0087	0.0093
e_ω	0.1812	0.1095	0.2503	0.1099
Computation time/ms	0.1520	0.8850	1.9088	1.200

TABLE 5. Precision and computation efficiency of four methods on a 48-machine 140-bus system.

Algorithms	EKF	CKF	EnKF	UKF
e_δ	0.1344	0.0101	0.0112	0.0096
e_ω	2.0644	0.1651	0.2402	0.1688
Computation time/ms	1.50	16.90	14.60	20.57

TABLE 6. The estimation accuracy of generator angles for four methods.

Rz	0	0.005	0.01	0.015	0.02	0.025	0.03
CKF	0	0.0034	0.0063	0.0080	0.0097	0.0120	0.0140
UKF	0	0.0034	0.0063	0.0078	0.0097	0.0120	0.0140
EnKF	0	0.0053	0.0075	0.0104	0.0140	0.0154	0.0202
EKF	0	0.0039	0.0068	0.0100	0.0132	0.0163	0.0178

Rz	0.035	0.04	0.045	0.05	0.055	0.06
CKF	0.0163	0.0184	0.0213	0.0222	0.0231	0.0261
UKF	0.0163	0.0184	0.0213	0.0222	0.0232	0.0260
EnKF	0.0217	0.0274	0.0284	0.0291	0.0324	0.0321
EKF	0.0227	0.0253	0.0286	0.0297	0.0332	0.0396

TABLE 7. The estimation accuracy of generator speeds for four methods.

Rz	0	0.005	0.01	0.015	0.02	0.025	0.03
CKF	0	0.0783	0.1068	0.1245	0.1405	0.0181	0.1848
UKF	0	0.0815	0.1065	0.1221	0.1398	0.1805	0.1850
EnKF	0	0.1057	0.1347	0.1772	0.2146	0.2396	0.3086
EKF	0	0.1825	0.2545	0.3277	0.3955	0.4496	0.4682

Rz	0.035	0.04	0.045	0.05	0.055	0.06
CKF	0.2145	0.2412	0.2869	0.2841	0.2675	0.3147
UKF	0.2141	0.2414	0.2878	0.2839	0.2666	0.3139
EnKF	0.3103	0.4078	0.3979	0.4121	0.4708	0.4633
EKF	0.5618	0.6130	0.6623	0.6915	0.7436	0.8224

The EKF algorithm shows high calculation efficiency but cannot be used for large-scale power systems due to the complicated Jacobian matrix calculation and the sensitivity to measurement errors and system sizes. Although the UKF algorithm is insensitive to measurement errors and system sizes, the parameter setting is dependent on experience, and at the same time, the calculation efficiency decreases with the size of power systems. With the relatively low sensitivity to measurement errors and system sizes, the EnKF algorithm may be used for the applications with low estimation accuracy. In contrast, the CKF algorithm shows the best performance among these algorithms in achieving high estimation accuracy and the insensitivity to measurement errors and system sizes.

Therefore, the work of this paper can facilitate selecting state estimation algorithms for the solution to the DSE problems under different applications.

APPENDIX

See Tables 3–7.

REFERENCES

[1] N. Zhou, D. Meng, Z. Huang, and G. Welch, "Dynamic state estimation of a synchronous machine using PMU data: A comparative study," *IEEE Trans. Smart Grid*, vol. 6, no. 1, pp. 450–460, Jan. 2015.

[2] K.-Y. Wang, G. Mu, and X.-Y. Chen, "Precision improvement and PMU placement studies on state estimation of a hybrid measurement system with PMUS," *Proc. CSEE*, vol. 21, no. 3, pp. 29–33, 2001.

[3] Y. Wang, Y. Sun, V. Dinavahi, K. Wang, and D. Nan, "Robust dynamic state estimation of power systems with model uncertainties based on adaptive unscented H_∞ filter," *IET Gener., Transmiss. Distrib.*, vol. 13, no. 12, pp. 2455–2463, Jun. 2019.

[4] H. Zhang, S. Liu, and M. Sun, *Theory and Application of Optimal State Estimation*. Harbin, China: Harbin Institute of Technology Press, 2019.

[5] D. Simon, *Optimal State Estimation: Kalman, H Infinity, and Nonlinear Approaches*. Beijing, China: National Defence Industry Press, 2013.

[6] Z. Huang, K. Schneider, and J. Nieplocha, "Feasibility studies of applying Kalman Filter techniques to power system dynamic state estimation," in *Proc. Int. Power Eng. Conf. (IPEC)*, 2007, pp. 376–382.

[7] X. Qin, T. Bi, and Q. Yang, "Dynamic state estimator based on WAMS during power system transient process," *Proc. CSEE*, vol. 28, no. 7, pp. 19–25, 2008.

[8] S. Akhlaghi, N. Zhou, and Z. Huang, "Exploring adaptive interpolation to mitigate non-linear impact on estimating dynamic states," in *Proc. IEEE Power Energy Soc. Gen. Meeting*, Jul. 2015, pp. 1–5.

[9] S. Akhlaghi and N. Zhou, "Adaptive multi-step prediction based EKF to power system dynamic state estimation," in *Proc. IEEE Power Energy Conf. Illinois (PECI)*, Feb. 2017, pp. 1–8.

[10] G. Valverde and V. Terzija, "Unscented Kalman filter for power system dynamic state estimation," *IET Gener., Transmiss. Distrib.*, vol. 5, no. 1, pp. 29–37, 2011.

[11] T. Bi, L. Chen, A. Xue, and Q. Yang, "A dynamic state estimation method considering speed governors," *Power Syst. Technol.*, vol. 37, no. 14, pp. 3433–3438, 2013.

[12] A. Ma, Q. Jian, H. Xiong, and H. Lu, "Dynamic state estimation method for generator considering measurement of bad data," *Autom. Electr. Power Syst.*, vol. 41, no. 14, pp. 140–146, 2017.

[13] L. Li, R. Li, and Y. Sun, "Power system dynamic state estimation with mixed measurements based on UKF," *Autom. Electr. Power Syst.*, vol. 34, no. 17, pp. 17–21, 2010.

[14] Z. Wei, G. Sun, and B. Pang, "Application of UKF and SRUKF to power system dynamic state estimation," *Proc. CSEE*, vol. 31, no. 16, pp. 74–80, 2011.

[15] J. Zhao and L. Mili, "Robust unscented Kalman filter for power system dynamic state estimation with unknown noise statistics," *IEEE Trans. Smart Grid*, vol. 10, no. 2, pp. 1215–1224, Mar. 2019.

[16] Z. Qu, Y. Dong, Y. Wang, and L. Chen, "Improved robust unscented Kalman filtering algorithm for dynamic state estimation of power systems," *Autom. Electr. Power Syst.*, vol. 42, no. 10, pp. 87–92, 2018.

[17] J. Qi, K. Sun, J. Wang, and H. Liu, "Dynamic state estimation for multi-machine power system by unscented Kalman filter with enhanced numerical stability," *IEEE Trans. Smart Grid*, vol. 9, no. 2, pp. 1184–1196, Mar. 2018.

[18] L. Chen, T. Bi, J. Li, A. Xue, Q. Li, and Q. Yang, "Dynamic state estimator for synchronous machines based on cubature Kalman filter," *Proc. CSEE*, vol. 34, no. 16, pp. 2706–2713, 2014.

[19] A. Sharma, S. C. Srivastava, and S. Chakrabarti, "A cubature Kalman filter based power system dynamic state estimator," *IEEE Trans. Instrum. Meas.*, vol. 66, no. 8, pp. 2036–2045, Aug. 2017.

[20] T. Bi, L. Chen, A. Xue, and Q. Yang, "Dynamic state estimator for synchronous machines based on robust cubature Kalman filter," *Trans. China Electrotech. Soc.*, vol. 31, no. 4, pp. 163–169, 2016.

[21] Y. Li, J. Li, J. Qi, and L. Chen, "Robust cubature Kalman filter for dynamic state estimation of synchronous machines under unknown measurement noise statistics," *IEEE Access*, vol. 7, pp. 29139–29148, 2019.

[22] X. Li, "The method of cubature Kalman filter and its application research," M.S. thesis, Dept. Comput. Inf. Eng., Henan Univ., Henan, China, 2016.

[23] Y. Li, Z. Huang, N. Zhou, B. Lee, R. Diao, and P. Du, "Application of ensemble Kalman filter in power system state tracking and sensitivity analysis," in *Proc. PES T&D*, May 2012, pp. 1–8.

[24] B. R. Hunt, E. J. Kostelich, and I. Szunyogh, "Efficient data assimilation for spatiotemporal chaos: A local ensemble transform Kalman filter," *Phys. D, Nonlinear Phenomena*, vol. 230, nos. 1–2, pp. 112–126, Jun. 2007.

[25] P. K. Ray and B. Subudhi, "Ensemble-Kalman-filter-based power system harmonic estimation," *IEEE Trans. Instrum. Meas.*, vol. 61, no. 12, pp. 3216–3224, Dec. 2012.

[26] G. Evensen, "The ensemble Kalman filter for combined state and parameter estimation," *IEEE Control Syst.*, vol. 29, no. 3, pp. 83–104, Jun. 2009.

[27] R. Huang, R. Diao, Y. Li, J. Sanchez-Gasca, Z. Huang, B. Thomas, P. Etingov, S. Kincic, S. Wang, R. Fan, G. Matthews, D. Kosterev, S. Yang, and J. Zhao, "Calibrating parameters of power system stability models using advanced ensemble Kalman filter," *IEEE Trans. Power Syst.*, vol. 33, no. 3, pp. 2895–2905, May 2018.

[28] G. Evensen, "The ensemble Kalman filter: Theoretical formulation and practical implementation," *Ocean Dyn.*, vol. 53, no. 4, pp. 343–367, Nov. 2003.

[29] R. Fan, Z. Huang, S. Wang, R. Diao, and D. Meng, "Dynamic state estimation and parameter calibration of a DFIG using the ensemble Kalman filter," in *Proc. IEEE Power Energy Soc. Gen. Meeting*, Jul. 2015, pp. 1–5.

[30] S. Liu and H. Mei, *Optimal Estimation Theory*. Beijing, China: Science Press, 2011.

[31] J. Chow and G. Rogers, "User manual for power system toolbox, version 3.0," Cherry Tree Sci. Softw., ON, Canada, Tech. Rep., 1991, pp. 11–40.

HUI LIU received the M.S. and Ph.D. degrees in power engineering from Guangxi University, Nanning, China, in 2017. He was a Postdoctoral Researcher of electrical engineering with Tsinghua University, Beijing, China, from 2011 to 2013. He is currently a Professor with the Department of Electrical Engineering, Guangxi University. His major research interest is power system control, electric vehicles, power system state estimation, and integrated energy systems.

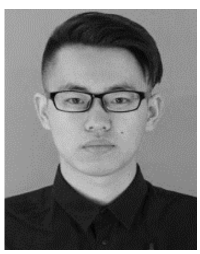

FEI HU received the B.E. degree in electrical engineering and automation from Southwest University, Chongqing, China, in 2018. He is currently pursuing the master's degree with the Department of Electrical Engineering, Guangxi University.

His major research interests are power system state estimation and application of artificial intelligence in electrical engineering.

JINSHUO SU was born in Nanning, Guangxi, China, in 1992. He received the B.E. degree in electrical engineering from the Hefei University of Technology, Hefei, China, in 2015. He is currently pursuing the Ph.D. degree in electrical engineering with the College of Electrical Engineering, Guangxi University. His research interest includes power system stability control.

XIAOWEI WEI received the B.E. degree in electrical engineering and automation from Hunan University, Hunan, China, in 2015, and the M.E. degree in electrical engineering from Guangxi University, Nanning, China, in 2019. He is currently working at Dongguan Power Supply Bureau, Guangdong Power Grid Corporation Ltd., Dongguan, China.

RISHENG QIN received the M.S. degree from the School of Electrical Engineering, Guangxi University, in 2005. He joined the Electric Power Research Institute, Yunnan Power Grid Corporation Ltd., in 2005. His research interests include reactive power analysis, voltage quality, power quality, and so on.